Authors: Hesterman, Novicki, White, Stokes, Cordova, Toddes, Silva, Burke, Domarkas, Wright, Archibald, Yost, Heimann, DiMagno, Hillier, Patel, Orcutt, Amor, Tully, Babich, Hoppin

Title:

Preclinical characterization of novel radiolabeled and fluorescent-labeled Fibroblast Activation Protein (FAP)-targeting ligands using gamma counting, SPECT imaging and Cryo-Fluorescence Tomography (CFT).

Aim/Introduction:

The emerging field of fluorescent-guided surgery represents a promising technique for tumor tissue imaging but has been hampered by a lack of clinically relevant pan-cancer imaging agents. Fibroblast activation protein is a potentially useful target to fill this gap. FAP is a type II membrane-bound glycoprotein enzyme with peptidase activity that is highly expressed on the cell surface of activated fibroblasts. It is highly expressed by cancer-associated fibroblasts which occur in the stroma of many cancers. FAP is expressed directly on the surface of some tumor cells as well as in remodeling processes where fibroblasts are activated such as wound healing, inflammation, and fibrosis.

FAP is increasingly used in clinical PET imaging. Development of analogous FAP fluorescent agents could lead to a clinical paradigm where FAP PET is used in conjunction with fluorescent-FAP guided surgical resection. The value of such complementary agents depends, in part, on consistency in biodistribution between the analogous PET and fluorescent compounds. Therefore, the aim of this study was to evaluate the relative biodistribution of a ZW800-1 fluorescent-labeled FAP compound and a 67Cu-labeled NOTA-conjugated FAP compound of otherwise analogous structure. The biodistribution of the FAP imaging candidate compounds was captured across multiple techniques, including radiolabeled gamma counting (GC), radiolabeled whole-body SPECT (SPECT), and whole-body cryo-fluorescence tomography (CFT).

Materials and Methods:

RTX-1363 and RTX-1341 are structurally similar compounds built on a trifunctional scaffold. Both exhibit sub-nanomolar enzymatic inhibition for human FAP (IC50s: 50 and 85 pM, respectively) with good selectivity (FAP/PREP >50). The major structural difference is the replacement of the N3O2 NOTA chelate in RTX-1363 with the optical dye ZW800-1 in RTX-1341. [67Cu]RTX-1363 was prepared by adding RTX-1363 in DMSO to a solution of Cu-67 in 0.05M HCl and adjusting the pH to 5.5 using 3N NaOAc. The mixture was heated for 15 minutes prior to assessing purity. Radiochemical purity was >95% using RP-HPLC.

A 1ug mass dose of either [67Cu]RTX-1363 or [ZW800-1]RTX-1341 was administered in 100 uL via tail-vain injection to U-87 MG tumor-bearing mice. Three animals were imaged longitudinally using SPECT/CT at 1h and 24h post-administration. Additional animals were

sacrificed at 1h or 24h post-administration for gamma counting or CFT imaging. Regions of interest were segmented from SPECT and CFT images, including tumor, knee joint, liver, and kidney. The liver was used as a reference region for semi-quantitative analysis.

Results:

Consistent biodistribution is observed across compounds through qualitative assessment and semi-quantitative analysis. Example maximum intensity projections (MIPs) for representative 1h time points are shown in Figure 1. No significant differences in macro tissue distribution were noted at any time point between the two methodologies. SPECT imaging enabled within-subject quantitative longitudinal assessment while CFT imaging provided higher resolution whole-body information, yielding insights such as the local distribution of the ligand on the surface of the bone and heterogeneity of distribution within the tumor as visualized in Figure 2. Semi-quantitative analysis, demonstrating the longitudinal intensity values relative to liver in tumor, knee joint, and kidney is shown in Figure 3.

Conclusion:

Strong agreement was observed in biodistribution between ZW800-1 fluorescent labeled and 67Cu radiolabeled compounds using gamma counting, whole-body SPECT and whole-body CFT. High-resolution *ex vivo* CFT imaging provided insights into local ligand distribution complementing low-resolution longitudinal *in vivo* SPECT data. Physiochemically similar characteristics between zwitter-ionic dye ZW800-1 and the Cu-N3O2 complex may have contributed to similarities in tissue biodistribution, further emphasizing that for certain ligands systems CFT could complement radiolabeled techniques for compound screening.

References:

1. Sutton, P. A., van Dam, M. A., Cahill, R. A., Mieog, S., Polom, K., Vahrmeijer, A. L., & van der Vorst, J. (2023). Fluorescence-guided surgery: comprehensive review. *BJS open*, *7*(3), zrad049.
2. Calais, J. (2020). FAP: the next billion dollar nuclear theranostics target?. *Journal of Nuclear Medicine*, *61*(2), 163-165.

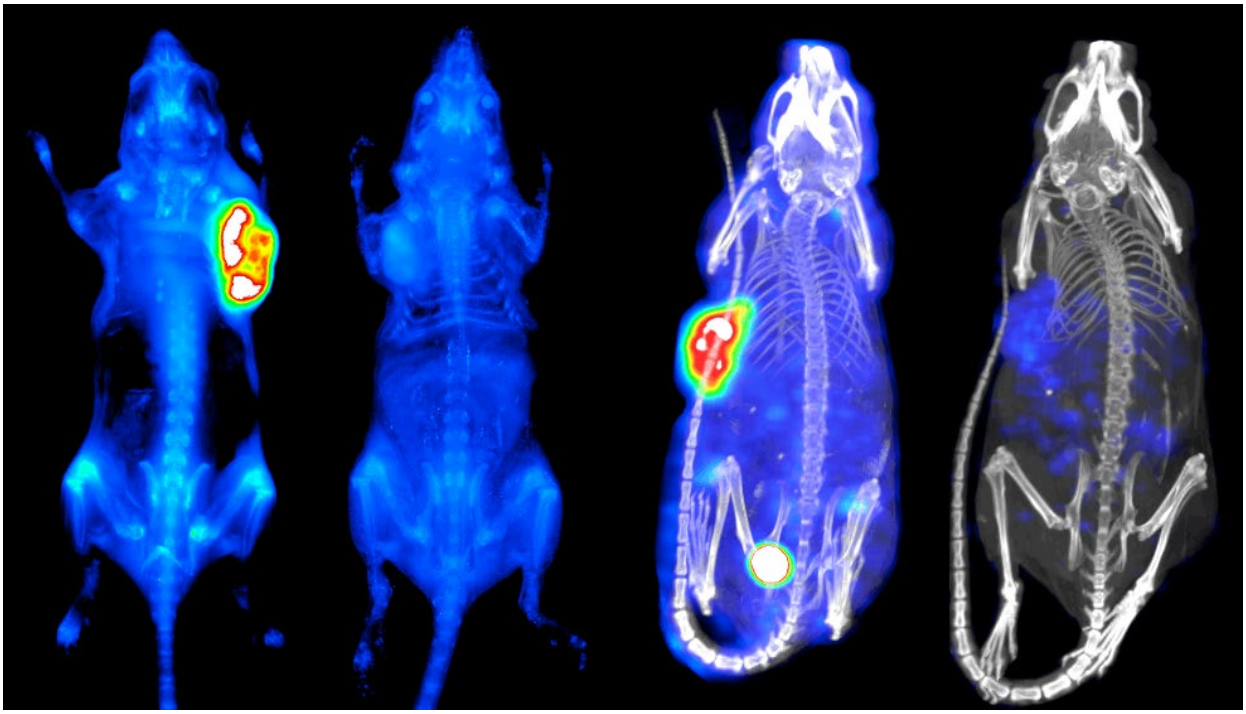

Figure 1: MIP images of (left-to-right) CFT at 1h, CFT at 24h, SPECT/CT at 1h, and SPECT/CT at 24h. All images are shown on a scale of 0-8, normalized to liver.

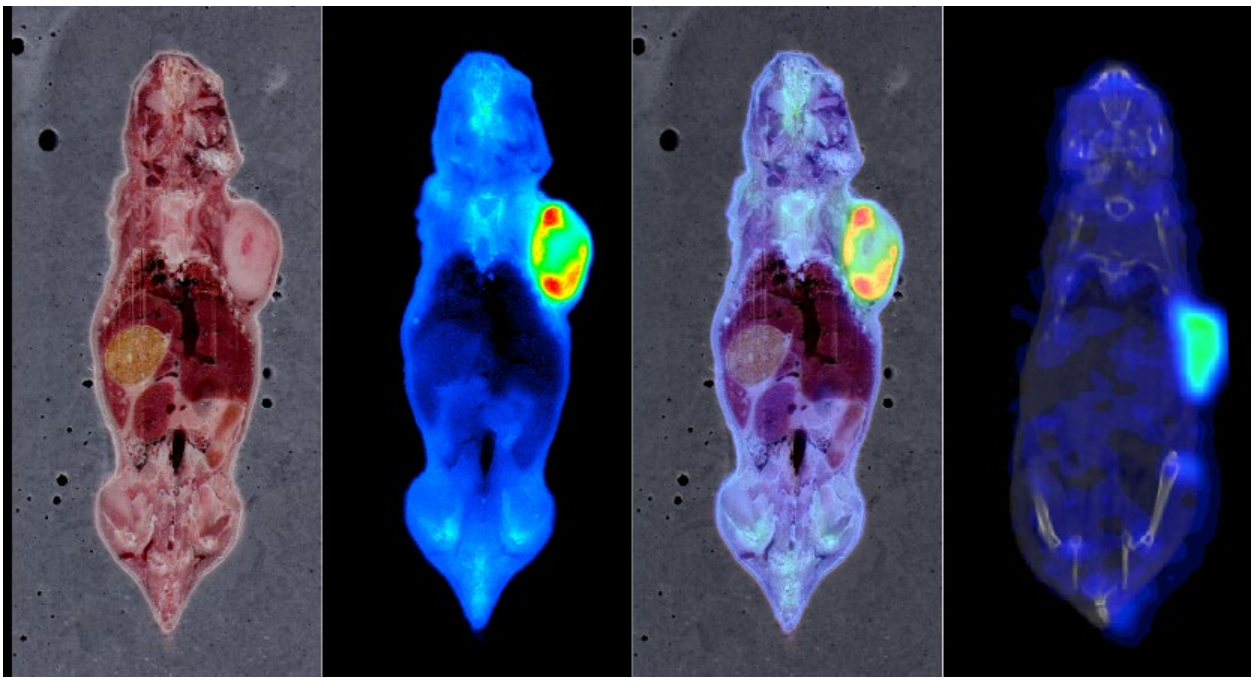

Figure 2: (left-to-right) White-light RGB, fluorescence, and merged image of a representative CFT slice. Representative SPECT/CT slice. All images are from 1h post-administration.

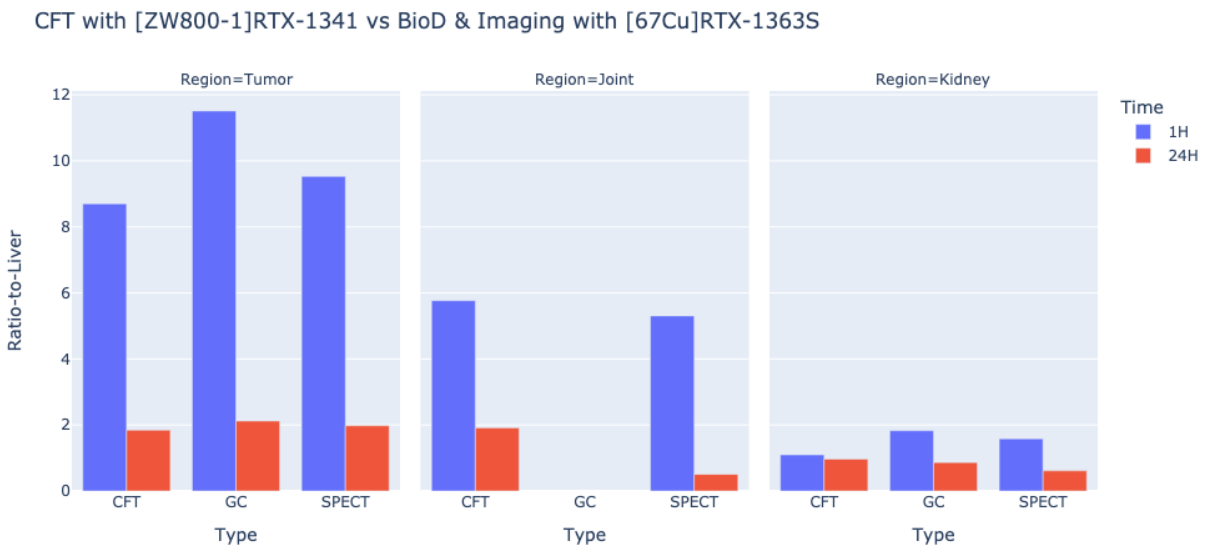

Figure 3: Semi-quantitative analysis of CFT, gamma counting, and SPECT data for tumor, knee joint, and kidney. Data are shown at 1h and 24h. All data are normalized to mean liver signal.